Environmental "Wiggles" as Stabilizers of Species Range Limits Set by Interspecific Competition

Farshad Shirani* Benjamin G. Freeman†

Abstract

Whether interspecific competition is a major contributing factor in setting species' range limits has been debated for a long time. Evolutionary models have helped propose a possible mechanism: interspecific competition interacts with the disruptive effects of gene flow along an environmental gradient to halt range expansion of species when they meet and compete with each other. However, the stability of such range limits has not previously been well-addressed. Here we use a deterministic evolutionary model to show that, when the environmental gradient varies linearly in space, range limits set by interspecific competition are unlikely to be evolutionarily stable. However, we demonstrate that step-like nonlinearities in the environmental optimum for a fitness-related phenotypic trait, or sharp changes in the steepness of the trait optimum, can stabilize competitively-formed range limits. We show that the stability of the range limits established at such nonlinearities is sufficiently robust against environmental perturbations such as climate change. We note that strong climatic changes can still destabilize the range limits, depending on how the relative dominance of the species changes across the environmental nonlinearities. Therefore, our results further highlight the importance of measuring the competitive ability of species when predicting their response to climate change.

Introduction

Why are species' range limits where they are? Understanding the reasons has been a longstanding challenge in spatial ecology (Bridle and Vines, 2007; Gaston et al., 2003; Miller et al., 2020; Sexton et al., 2009; Wallace, 1876). Developing such an understanding helps address a fundamental question about the future of biodiversity on the planet: where will the species' range limits be in

*School of Mathematics, Georgia Institute of Technology, Atlanta, GA 30332, USA
†School of Biological Sciences, Georgia Institute of Technology, Atlanta, GA 30332, USA

the near and far future? It is important, for instance, to know whether the currently contracting or expanding range of a species will eventually reach an evolutionarily stable equilibrium. This equilibrium could correspond to the species' complete exclusion from the habitat, its full expansion over the entire available habitat, or its existence with a limited range. In the latter case, it is important to foresee where the species' equilibrium range limits will be, whether or not they will return to the same equilibrium locations after being perturbed by changes in climate, or if they will completely be destabilized by particular climate changes. Using a mathematical model, we theoretically address some of these questions for the case where range limits are formed by interspecific competitions and are stabilized by certain environmental nonlinearities.

Since Darwin, ecologists have debated the role of interspecific competition in setting species' range limits (Connell, 1983; Darwin, 1859; Louthan et al., 2015; Schoener, 1983; Wisz et al., 2013). Empiricists have used experiments and comparisons to test whether competition can limit species' ranges (Connell, 1961; Diamond, 1985; Freeman et al., 2022; Hairston, 1980), while theoreticians have developed mathematical models to explore the conditions in which interspecific competition can set range limits (Case and Taper, 2000; Case et al., 2005; Goldberg and Lande, 2006; Price and Kirkpatrick, 2009; Roughgarden, 1979; Shirani and Miller, 2022; Tilman, 1982). The model developed by Case and Taper (2000) has been especially influential. They particularly demonstrate that the interaction between interspecific competition and gene flow can set stable range limits along environmental gradients. However, phenotypic variance is constant over space and time in their model, an assumption Case and Taper (2000) describe as "tenuous". In addition, the stability of the range limits in their two-species simulations is established for identical competitors, which is unlikely to ever be the case in nature. Here, we address these limitations to explore how interspecific competition can interact with spatial changes in environmental gradients to set stable range limits under more realistic conditions.

We particularly aim to investigate the stability of range limits formed by interspecific competition, and whether or not it is robust against changes in the environment. The stability of the range limits demonstrated by Case and Taper (2000) for two identical competitors is non-generic, that is, the limits are not stable if one of the species is competitively stronger than the other. Even for the unlikely case of competitively identical species, the limits in Case and Taper's results are not stable in stricter senses of stability. If the coevolutionary equilibrium ranges of the species are perturbed by a sustained (non-vanishing) change in the environment, they do not return to their original equilibrium state even after both species adapt to the new environment. It thus remains unclear if interspecific competition can set stable range limits that meet sufficiently strict senses of stability. We focus on one reasonable stabilizing factor—relatively sharp step-like undulations, or "wiggles" as we call them, in the spatial profile of the environmental optimum for a fitness-related quantitative trait. Such wiggles are likely pervasive in the real world, as nonlinear spatial changes in climate, geology, habitat structure, or biotic communities are commonly observed along environmental gradients. We provide quantitative theoretical support for the hypothesis that wiggles are important stabilizers of range limits formed by interspecific competition.

To accomplish our goals, we use a mathematical model of species' range evolution developed by

Shirani and Miller (2022) as an extension of the seminal works of Kirkpatrick and Barton (1997) and Case and Taper (2000). This model allows for joint evolution of the population density and the intraspecific mean and variance of a quantitative phenotypic trait for each of the species in a community of competitively interacting species. The intra- and inter-specific competitions between the species' individuals in the model are phenotype-dependent, which subject the individuals to frequency-dependent selection. The phenotypic trait is assumed to be strongly correlated with individuals' fitness. The model incorporates the effects of directed and stabilizing natural selection, which act to gradually reduce the density of the phenotypes that differ from an optimum phenotype imposed by the environment. We model an environmental wiggle by sharply changing the slope of the spatial profile of this environmental optimum trait over a short geographic region. We perform numerical simulations for two related species, one being competitively stronger than the other. We explore the evolution of the species' competitively formed range limits as they enter and get stabilized in an environmental wiggle. We test the robustness of the range limits established at a wiggle against moderate and strong climate-warming perturbations.

Methods

We obtain our results by numerically solving the equations of the model developed by Shirani and Miller (2022), which is a system of partial differential equations capturing the eco-evolutionary dynamics of species' ranges in a community of species in a heterogeneous environment. The model has been developed in a quantitative genetic framework, wherein evolution occurs based on the value of a fitness-related phenotypic trait that each individual in the community possesses. Populations are assumed to be fully polymorphic. All phenotypes are assumed to be present in each population at all time, with different frequencies. Evolution proceeds by differential growth of the phenotypes under the selective load of frequency-dependent phenotypic competition as well as the genetic load imposed by natural selection. Here, we only present the equations and the essential components of a reduced version of Shirani and Miller's model for two interacting species in a one-dimensional geographic space. We refer the reader to their work for further details of the model for multiple species in higher dimensional spaces.

Model Components

We present the components of the model for adaptive range evolution of two species in a one-dimensional habitat, over an evolution time horizon from $t = 0$ to $t = T > 0$. We denote the habitat by an open interval $\Omega = (a, b) \subset \mathbb{R}$. At every location $x \in \Omega$ and time $t \in [0, T]$, the ith species' range dynamics is governed by three coupled equations that control the joint evolution of the population density $n_i(x, t)$, intraspecific trait mean $q_i(x, t)$, and intraspecific trait variance $v_i(x, t)$, where $i = 1, 2$. Before presenting the final equations of the model in the next section, we describe its basic contributing components as follows.

Let $\phi_i(x, t, p)$ denote the relative frequency of phenotype value $p \in \mathbb{R}$ within the ith species'

population. Then $n_i(x,t)\phi_i(x,t,p)$ gives the population density of individuals with phenotype p in the ith population. The model assumes that changes in $n_i(x,t)\phi_i(x,t,p)$ over a small time interval of $\tau \to 0$ results from the contribution of three major factors, given by:

$$
\begin{aligned}
n_i(x,t+\tau)\phi_i(x,t+\tau,p) - n_i(x,t)\phi_i(x,t,p) & \\
= \tau \mathrm{D}\, \partial_x^2 (n_i(x,t)\phi_i(x,t,p)) & \quad (1a)\\
+ \tau g_i(x,t,p) n_i(x,t)\phi_i(x,t,p) & \quad (1b)\\
+ \tau n_i(x,t)\partial_t^{(\mathrm{M})}\phi_i(x,t,p), & \quad (1c)
\end{aligned}
$$

where ∂_x^2 denotes the second partial derivative with respect to x. The first contributing factor (1a) represents the diffusive (random) dispersal of individuals to and from neighboring locations, where D denotes the diffusion coefficient. The second contribution (1b) is due to the intrinsic growth of the individuals with phenotype p in the ith population, the rate of which is denoted by $g_i(x,t,p)$. Finally, the third factor (1c) represents mutational changes in the relative frequency of the phenotype p, occurring at a rate denoted by $\partial_t^{(\mathrm{M})}\phi_i(x,t,p)$. The probability of mutational changes from a phenotype p to another phenotype p' is assumed to be dependent on the difference $\delta p = p - p'$ between the phenotypes. Letting $\nu(\delta p)$ denote the probability density of the occurrence of such mutational changes, the model further assumes that ν follows a distribution with zero mean and constant variance. Based on these assumptions, the formulation used in the model for $\partial_t^{(\mathrm{M})}\phi_i(x,t,p)$ is given in Section A.3 of the work by Shirani and Miller (2022).

The key factor that differentiates the density of individuals with different phenotypes is their intrinsic growth rate, which is modeled as (Shirani and Miller, 2022: Equ. (17)),

$$
\begin{aligned}
g_i(x,t,p) := \mathrm{R}_i \left(1 - \frac{1}{\mathrm{K}_i}\sum_{j=1}^{2} n_j(x,t)\int_{\mathbb{R}} \alpha_{ij}(p,p')\phi_j(x,t,p')\mathrm{d}p'\right) & \quad (2a)\\
- \frac{\mathrm{S}}{2}(p - \mathrm{Q}(x))^2, & \quad (2b)
\end{aligned}
$$

where R_i denotes the maximum growth rate of the ith species, K_i denotes the carrying capacity of the environment for the ith species, S denotes the strength of stabilizing selection, and $\mathrm{Q}(x)$ denotes the environment's optimal trait value at location x. The convolution term in the Lotka-Volterra term (2a) models the effects of phenotypic competition between the individuals. Specifically, the competition kernel $\alpha_{ij}(p,p')$ denotes the strength of the per capita effects of individuals with phenotype p' in the jth species on the frequency of individuals with phenotype p in the ith species. In writing (2a), it is essentially assumed that the reproduction rate of the individuals with phenotype p follows a logistic growth, with the carrying capacity and maximum growth rate of individuals being independent of their phenotype.

For the competition kernel $\alpha_{ij}(p,p')$, the model uses the MacArthur-Levins overlap (Macarthur and Levins, 1967) between *phenotype utilization curves* of the individuals. For this, the environmental resources are assumed to vary continuously along a resource axis. The probability that the individuals obtain a unit of resource from a point on the resource axis defines the individuals' resource utilization curve. It is further assumed that there is a one-to-one map between the resource

axis and the phenotype axis. Using this map, the resource axis is identified by the phenotype axis and the individuals' resource utilization curves are replaced with phenotype utilization curves (Roughgarden, 1979: Eq. (24.5)). The phenotype utilization distribution (curve) associated with individuals with phenotype p in the ith population is then assumed to be normal, with mean p and constant utilization variance V_i; see (Shirani and Miller, 2022: Equ. 22). Finally, the overlap between the phenotype utilization curves gives the competition kernel as

$$\alpha_{ij}(p,p') = \sqrt{\mathrm{V}_i/\bar{\mathrm{V}}_{ij}}\exp\left(-\frac{(p-p')^2}{4\bar{\mathrm{V}}_{ij}}\right), \tag{3}$$

where $\bar{\mathrm{V}}_{ij} := \frac{1}{2}(\mathrm{V}_i + \mathrm{V}_j)$. The details are given in Sections A.2 and A.4 of the work by Shirani and Miller (2022).

The quadratic term (2b) in the intrinsic growth function imposes directional and stabilizing forces of natural selection on individuals with phenotype p. It penalizes phenotypes that are far from the environmental optimal phenotype $\mathrm{Q}(x)$, thereby facilitating adaptation to new environments. In our results, we model environmental wiggles by inserting short-range undulations in the otherwise linear profile of Q.

The phenotype density evolution equation (1), along with the definition of its components as described above, is used to derive the final equations of the model for the evolution of n_i, q_i, and v_i. The derivation of the equations (Shirani and Miller, 2022) relies on a key assumption: phenotype values in each species are normally distributed at every occupied habitat location for all time (Case and Taper, 2000; Kirkpatrick and Barton, 1997). This assumption allows for exact moment closure in deriving the equations for trait means and trait variances. It is argued by Barton (2001; 1999) that this assumption is fairly reasonable when the majority of genetic variation in the species is maintained by gene flow rather than by mutation. The analysis performed by Shirani and Miller (2022) shows that this is indeed the case when species' ranges adaptively evolve in sufficiently steep environmental gradients—which is a condition that holds in all of the simulations we perform in this work.

Model Equations

The model is specified by a system of partial differential equations for the evolution of each species' population density $n_i(x,t)$, trait mean $q_i(x,t)$, and trait variance $v_i(x,t)$ at every habitat location $x \in \Omega$ and time $t \in [0,T]$, $T > 0$. For brevity, let $u := (n_1, q_1, v_1, n_2, q_2, v_2)$ be a vector containing all model variables. Moreover, let the partial derivative with respect to t and x be denoted by ∂_t and ∂_x, respectively, and the second partial derivative with respect to x be denoted by ∂_x^2. Then, the equation for the evolution of the population density n_i of the ith species is given by

$$\partial_t n_i(x,t) = \mathrm{D}_i \partial_x^2 n_i(x,t) + G_i(x, u(x,t)) n_i(x,t), \tag{4}$$

where $G_i(x,u)$ denotes the mean growth rate of the population as given by (7) below. Likewise, equations for the evolution of trait mean q_i and trait variance v_i within the ith species are given

as

$$\partial_t q_i(x,t) = \mathrm{D}_i \partial_x^2 q_i(x,t) + 2\,\mathrm{D}_i \partial_x\big(\log n_i(x,t)\big)\partial_x q_i(x,t) + H_i(x,u(x,t)), \tag{5}$$

and

$$\begin{aligned}\partial_t v_i(x,t) = \mathrm{D}_i \partial_x^2 v_i(x,t) + 2\,\mathrm{D}_i \partial_x\big(\log n_i(x,t)\big)\partial_x v_i(x,t)\\ + 2\,\mathrm{D}_i\big(\partial_x q_i(x,t)\big)^2 + W_i(x,u(x,t)).\end{aligned} \tag{6}$$

The nonlinear mappings G_i, H_i, and W_i used in (4)–(6) are defined as

$$G_i(x,u) = \mathrm{R}_i - \frac{\mathrm{R}_i}{\mathrm{K}_i}\sum_{j=1}^{2} M_{ij}(u)C_{ij}(u)n_j - \frac{\mathrm{S}}{2}\left[\big(q_i - \mathrm{Q}(x)\big)^2 + v_i\right], \tag{7}$$

$$H_i(x,u) = \big(\mathrm{R}_i - G_i(x,u)\big)q_i - \frac{\mathrm{R}_i}{\mathrm{K}_i}\sum_{j=1}^{2} L_{ij}(u)M_{ij}(u)C_{ij}(u)n_j + E_i(x,u), \tag{8}$$

$$W_i(x,u) = \big(\mathrm{R}_i(x) - G_i(x,u)\big)\big(v_i - q_i^2\big) - \frac{\mathrm{R}_i}{\mathrm{K}_i}\sum_{j=1}^{2} P_{ij}(u)M_{ij}(u)C_{ij}(u)n_j + Y_i(x,u), \tag{9}$$

where, letting $\bar{\mathrm{V}}_{ij} := \frac{1}{2}(\mathrm{V}_i + \mathrm{V}_j)$, $i,j \in \{1,2\}$,

$$C_{ij}(u) := \sqrt{\frac{2\mathrm{V}_i}{v_i + v_j + 2\bar{\mathrm{V}}_{ij}}}, \tag{10}$$

$$M_{ij}(u) := \exp\left(-\frac{(q_i - q_j)^2}{2(v_i + v_j + 2\bar{\mathrm{V}}_{ij})}\right), \tag{11}$$

$$L_{ij}(u) := \frac{v_i q_j + (v_j + 2\bar{\mathrm{V}}_{ij})q_i}{v_i + v_j + 2\bar{\mathrm{V}}_{ij}}, \tag{12}$$

$$P_{ij}(u) := \frac{v_i(v_j + 2\bar{\mathrm{V}}_{ij})}{v_i + v_j + 2\bar{\mathrm{V}}_{ij}} + L_{ij}(u)(L_{ij}(u) - 2q_i), \tag{13}$$

$$E_i(x,u) := \frac{\mathrm{S}}{2}\left[2\mathrm{Q}(x)v_i + 2\mathrm{Q}(x)q_i^2 - \mathrm{Q}^2(x)q_i - 3v_i q_i - q_i^3\right], \tag{14}$$

$$Y_i(x,u) := \frac{\mathrm{S}}{2}\left[2\mathrm{Q}(x)v_i q_i - 2\mathrm{Q}(x)q_i^3 - \mathrm{Q}^2(x)(v_i - q_i^2) - 3v_i^2 + q_i^4\right] + \mathrm{U}. \tag{15}$$

Solving the equations of the model (4)–(6) over a habitat $\Omega = (a,b)$ requires specifying boundary conditions at habitat boundary points $x = a$ and $x = b$. For our numerical studies presented in the Results section we always assume that there is no phenotypic flux through the boundary of the habitat, which gives the homogeneous Neumann boundary conditions

$$\partial_x n_i = 0, \quad \partial_x q_i = 0, \quad \partial_x v_i = 0, \quad i = 1,\ldots,\mathrm{N} \qquad \text{on } \{a,b\}\times[0,T]. \tag{16}$$

Equivalently, these conditions imply that the habitat boundary is reflecting.

Table 1 gives the definitions of the model parameters and their default values used in our simulations. The choice of units for the physical quantities of the model is an important factor in suggesting biologically reasonable values for model parameters based on available estimates in the literature. Due to the complexity of the equations, analytical studies of the behavior of the

Table 1: Definition and default values of the parameters of the model (4)–(6). The default values are used in the simulations presented in the Results section, unless otherwise is stated. The default value "Linear" specified for Q means that Q is by default considered to be a linear function of x over Ω.

Parameter	Definition	Default	Unit
D_i	Diffusion coefficient of the ith species' dispersal	1	$\mathtt{X}^2/\mathtt{T}$
K_i	Carrying capacity of the environment for ith species	1	$\mathtt{N}/\mathtt{X}^{\mathrm{m}}$
R_i	Maximum population growth rate of ith species	1	$1/\mathtt{T}$
V_i	Variance of individuals' phenotype utilization in ith species	4	$\mathtt{Q}^2$
S	Measure of the strength of stabilizing selection	0.2	$\mathtt{Q}^{-2}/\mathtt{T}$
U	Rate of increase in trait variance due to mutation	0.02	$\mathtt{Q}^2/\mathtt{T}$
$\mathrm{Q}(x)$	Optimal trait value for the environment	Linear	$\mathtt{Q}$
$\lvert \mathrm{d}_x\mathrm{Q}(x)\rvert$	Magnitude of the gradient of the optimal trait	0.5	$\mathtt{Q}/\mathtt{X}$

model in different evolutionary regimes will be rather impractical. Numerical studies of the model, as we perform in this work, will then require carefully chosen parameter values such that the resulting predictions are sufficiently reasonable. An extensive discussion is made by Shirani and Miller (2022) on the choice of units and reasonable ranges of parameter values. Below, we only describe the choices of units as needed for understanding the values given in Table 1.

Parameter Units

To specify units for the physical quantities of the model, one of the species in the community is first chosen as a *representative species*, for example, the one which is best adapted to the environment or has widest niche. The units are then specified based on the measurements made on the representative species. Specifically, the unit of time, denoted by $\mathtt{T}$, is set to be equal to the mean generation time of the representative species. The unit of space, denoted by $\mathtt{X}$, is chosen such that the diffusion coefficient D of the representative population becomes unity. That is, $1\,\mathtt{X}$ is set to be equal to the root mean square of the dispersal distance of the population in $1\,\mathtt{T}$, divided by $\sqrt{2}$. Having set the unit of space, the unit of measurement for population abundances, $\mathtt{N}$, is then chosen such that $1\,\mathtt{N}$ is equal to the carrying capacity of the environment for $1\,\mathtt{X}$ unit of habitat length. Note that this results in the default value of the carrying capacity for the representative population to become unity. Finally, letting $\mathtt{Q}$ denote the unit of measurement for the quantitative trait, $1\,\mathtt{Q}$ is set to be equal to one standard deviation of the trait values at the core of the representative population.

Results

We investigate how the interaction between interspecific competition and gene flow leads to formation of range limits, and how the limits are stabilized by environmental wiggles. For this, we numerically solve the equations of the model (4)–(6) for two competing species, with the nonlinear terms given by (7)–(15). To demonstrate character displacement and formation of range limits, we first characterize the two species with identical ecological and evolutionary parameter values, equal to the default values given in Table 1. We then make specific changes in the maximum growth rate of each species to further investigate the more generic case of competitively non-identical species.

We perform our simulations in the one-dimensional habitat $\Omega = (0\,\mathtt{X}, 70\,\mathtt{X}) \subset \mathbb{R}$ with the reflecting boundary conditions (16). We set the spatial profile of the trait optimum Q to be decreasing along the habitat. We can conceptualize this simplified habitat to represent, for example, the living environment of two species of montane birds over an elevation-dependent temperature gradient, with Q representing a temperature-correlated phenotypic trait. The reflecting boundary condition at $x = 70$ can then be equivalent to symmetrically (reflectively) expanding the habitat at the mountain top. Our choice of the default value $\mathrm{R}_i = 1\ \mathtt{T}^{-1}$ in Table 1 is also purposed to agree with a typical value of maximum growth rate per generation for birds (Dillingham et al., 2016; Niel and Lebreton, 2005; Shirani and Miller, 2022).

In all simulations, we initially introduce the two populations allopatrically, considering the 1st population as the *downstream* (at lower elevations) and the 2nd population as the *upstream* species. We assign the initial population densities at $t = 0\ \mathtt{T}$ as $n(x, 0) = 0.5\,\mathrm{sech}(|x - c_i|)$, where c_i denotes the center of the ith population. We assume that the initial populations are perfectly adapted to their environment at their center, that is, $q_i(c_i, 0) = \mathrm{Q}(c_i)$. However, we assume fairly poor initial adaptation at other habitat locations, by letting the slope of the initial trait means vary as $\partial_x q_i(x, 0) = 0.1\,\partial_x \mathrm{Q}(x)$, for all $x \in \Omega$. Finally, we assume that the initial populations have a constant trait variance of $v_i(x, 0) = 1\ \mathtt{Q}^2$.

Interspecific Competition, Asymmetric Gene Flow, and Formation of Species' Range Limits

Interspecific competition and gene flow along an environmental gradient can jointly contribute to the evolution of character displacement and range limits when two species become sympatric over a habitat region. For competitively identical species, this was first shown by Case and Taper (2000) under the constant (in time and space) trait variance assumption, and then confirmed by Shirani and Miller (2022) for the case where trait variance is free to evolve. Here, we briefly demonstrate these predictions to establish the framework for our further investigations of the stability of the range limits. We initialize the two species with identical parameters at opposite sides of the habitat, and compute their range evolution under different levels of the steepness of the environmental gradient. The results are shown in Figure 1.

When environmental gradient is sufficiently steep, we observe that range limits are formed

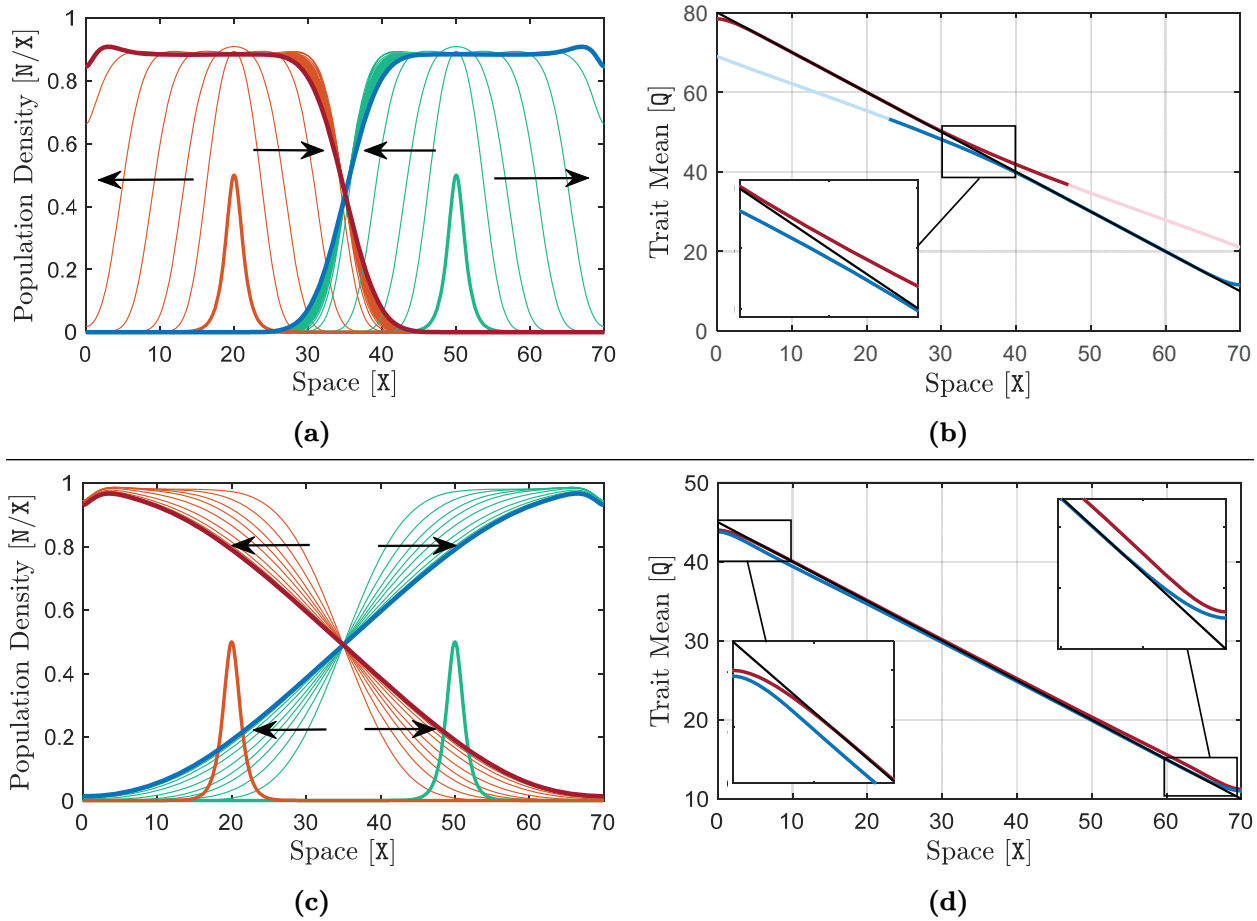

Figure 1: Evolution of character displacement and regions of sympatric coexistence for two competitively identical species. Both species have the same parameter values equal to the default values given in Table 1. The trait optimum Q is linear and decreasing, shown by the black lines in (b) and (d). Graphs (a) and (b) in the upper panel are associated with a simulation with a sufficiency steep environmental gradient of $\partial_x \mathrm{Q} = -1$ Q/X. Graphs (c) and (d) in the lower panel are associated with a simulation with a shallower gradient of $\partial_x \mathrm{Q} = -0.5$ Q/X. Curves of the species' population density, as their range evolves in time, are shown in (a) and (c). For the downstream (left) species, curves are shown in orange, thick orange curves indicate the initial curves at $t = 0$ T, and the final curves at the end of the simulation are highlighted in red. For the upstream (right) species, curves are shown in green, thick green curves indicate the initial curves, and the final curves are highlighted in blue. Arrows show the direction of evolution in time. In (a), curves are shown are shown at every 10 T for a simulation time horizon of $T = 1000$ T. A limited region of sympatry is formed at the middle of the habitat in about 40 T, and approximately remains unchanged afterwards. In (b), curves are shown at every 500 T for a simulation time horizon of $T = 5000$ T. The region of sympatry formed at the middle of the habitat continues to expand, rather slowly, until the species become completely sympatric over the entire habitat, in about 4000 T. The final curves of the species' trait mean obtained at the end of the simulations are shown in (c) and (d). The curves are made transparent over the regions where population densities are approximately zero, as the values of trait mean over these regions are not biologically meaningful. In both simulations, the species evolve character displacement over the region of sympatry.

around the interface of the two species. The initially allopatric species adapt to new habitat locations and expand their range. They become sympatric over a small region when they first meet at the middle of the habitat. Since both species are relatively well-adapted to the environment when they meet, their individuals over the region of sympatry have close phenotypes. This initiates a strong interspecific competition between the individuals, and induces character displacement over the region of sympatry. The character displacement further implies departure of the trait mean of each species from the trait optimum. The resulting maladaptation, along with the effects of interspecific competition, substantially decreases the population density of the two species at their interface (Figure 1a). This decline in density further increases the asymmetry in the core-to-edge gene flow within each species, from their populous center to their low-density peripheral populations at the interface of the two species. This asymmetric gene flow is maladaptive and, due to the term $2\,\mathrm{D}_i\partial_x(\log n_i)\partial_x q_i$ in (5), moves the species' trait mean further apart from the optimum trait over the region of sympatry. As the spatial overlap between the two species increases, the reinforcing feedback between character displacement and asymmetric gene flow continues to induce further maladaptation and decline in density, until the level of maladapted phenotypes at each species' interfacing edge with the other species becomes so strong that prevents further local adaptation and range expansion. As a result, a range limit is established for each species and a region of sympatry is formed between the species at the middle of the habitat. The highlighted curves in Figures 1a and 1b show the steady-state population densities and trait means, respectively. Further details, including the spatial evolution of trait variances, can be found in Figure 7 of the work by Shirani and Miller (2022). We further note that, although not shown here, intraspecific trait variance declines within each species over the region of sympatry. This reduced variation in phenotypes indeed allows for the evolution of sufficiently strong character displacement and maladaptation, as required for establishment of the range limits.

When environmental gradient is not sufficiently steep, the maladaptive effects of asymmetric gene flow cannot reinforce character displacement to the level required to stop range expansion of the species within a finite sympatric region. As Figures 1c and 1d show, in this case the overlap between the species continues to expand and the species eventually become completely sympatric over the entire available habitat. The evolution of this entire sympatry is, however, much slower than the evolution of the limited sympatry in Figure 1a.

Finally, we note that the evolution of character displacement requires the diversifying selection generated by competitive interactions between phenotypes to be sufficiently stronger than stabilization selection (Case and Taper, 2000). The character displacements shown in Figures 1b and 1d become more pronounced if the strength of stabilization selection S decreases (Case and Taper, 2000: Figure 5), or if phenotypic competition is intensified by increasing V_1 and V_2. Simulations performed by Shirani and Miller (2022) for faster growing species ($\mathrm{R}_1 = \mathrm{R}_2 = 2\ \mathtt{T}$) also show stronger levels of character displacement. Here, we perform our simulations with (relatively) slowly growing species to follow our conceptualization of the range evolution of montane birds.

Range Limits in Linear Environments: Stable or Unstable?

The range limits formed in Figure 1a—for competitively identical species in a linear environment—are identified as evolutionarily stable limits by Case and Taper (2000). This identification is due to the fact that the partially sympatric distribution of the two species eventually converges to a coevolutionary equilibrium (steady state) as $t \to \infty$. At this equilibrium state, to which the initially allopatric species converge asymptotically, both species have a limited range.

We first note that, although the equilibrium state in Figure 1a can be identified as stable in mathematical sense, it is not asymptotically stable. If, for example, we initialize the downstream species at the same location as in Figure 1a, but displace the initial population of the upstream species upward, then the distribution of the two species will converge to a different equilibrium, no matter how small the displacement of the initial upstream species is. This new equilibrium will look essentially the same as the equilibrium shown in Figure 1a, but with a region of sympatry and range limits that are shifted upward.

We further note that, in a stricter sense of stability, the equilibrium state in Figure 1a fails to persist against sustained perturbations in the environment, such as climate change, no matter how small they are. To see this, we initialize our simulation with the equilibrium populations of Figure 1a, and then gradually shift up the line of trait optimum by a factor of 5 $\mathtt{Q}$ over a time course of 10 $\mathtt{T}$. We then keep the trait optimum unchanged for the rest of the simulation ($T = 200$ $\mathtt{T}$). We can conceptualize this perturbation, for example, as a steady change in the environment due to climate warming. The simulation results are shown in the supplementary Figure S1. We observe that, due to the climate-warming perturbation, the equilibrium distribution of Figure 1a is shifted upslope, resulting in a shift in the species' range limits. Since $\partial_x \mathrm{Q} = -1$ $\mathtt{Q}/\mathtt{X}$, the spatial shift in the range limits due to the 5 $\mathtt{Q}$ shift in the trait optimum appears to be exactly equal to 5 $\mathtt{Q}$. This direct proportionality further implies that, the range limits formed in Figure 1a will not be restored to their original location when a sustained change occurs in climate, no matter how small the change is. It should be noted though, that the original range limits will be restored if the environmental changes appear as transient fluctuations, such that the trait optimum line is temporarily shifted up or down but eventually returns exactly to its original value. Such transient perturbations that completely vanish in time, unless large in amplitude, may not be of particular interest in studying stability of range limits.

More importantly, when the environment is linear, the stability of the limited ranges formed by interspecific competition is non-generic. That means, a coevolutionary equilibrium state such as the one shown in Figure 1a—with a fraction of each species' range being sympatric and the remaining being allopatric—almost never exists. The equilibrium state in Figure 1a exists only for the very specific case of "identical" competitors, which is unlikely to ever be the case in the real world. If one of the species is competitively stronger than the other, it constantly pushes the interface between the two species toward the weaker species. Simulations then predict two possible evolutionary outcomes: complete exclusion of the weaker species, or marginal existence of the weaker species at the vicinity of the habitat boundary.

When one of the species is much stronger than the other, it totally dominates the habitat and results in complete exclusion of the other species. This is shown in Figure 2a, where the downstream species is dominant due to its significantly larger maximum growth rate ($R_1 = 1.2\ \mathtt{T}^{-1}$ versus $R_2 = 1\ \mathtt{T}^{-1}$).

When the difference between the two species is less significant, as in Figure 2b, an evolutionarily stable state of marginal coexistence can eventually form as the interface between the two species approaches the habitat boundary. In this case, the weaker species survives with a limited density at close vicinity of the boundary. This is because when this species is eventually pushed against the boundary, it starts gaining advantage from its range contraction and density decline. Since there is no influx of phenotypes from the boundary, the contraction in range results in less genetic load (due to gene flow) on the peripheral population of this species at its interface with the stronger species. Additionally, the decrease in density reduces the intraspecific competition load on the population. The stronger species, however, does not enjoy these advantages. As a result, the decrease in the fitness load on the weaker species compensates for this species' moderate weakness in interspecific competition and allows the species to survive.

Based on the discussion above, we argue that when the environment changes linearly in space, range limits formed by the interaction between interspecific competition and gene flow are unlikely to be evolutionarily stable. Below, we show how environmental wiggles, as special types of plausible environmental nonlinearities, can effectively stabilize such range limits. For the non-generic case of identical competitors, Case and Taper (2000) have shown that the transition zone between the two species will often become "attached" to places where such nonlinearities exist. We perform our analysis for the general case of non-identical competitors and investigate the stability of the range limits in a fairly strict sense. More specifically, we show that environmental wiggles can stabilize competitively-formed range limits as a coevolutionary equilibrium, and we further show that the stability of this equilibrium is sufficiently robust against sustained climatic changes in the environment, such as permanent climate warming.

Environmental Wiggles Can Stabilize Range Limits

We define an environmental wiggle as a step-like spatial undulation (nonlinearity) in the environmental trait optimum, across which an initially moderate slope (magnitude of the gradient) of the trait optimum changes sharply to a significantly steeper slope followed by another change back to a moderate slope. We further require the spatial span of this undulation to be short, relative to the mean dispersal distance of the individuals. The undulation shown in the curve of trait optimum in Figure 3a is an example of a wiggle. According to this definition, a wiggle will be a nonlinearity along the environmental gradient with two "knees", which are the places where the sharp transitions in the slopes occur. We should note that, the steep abiotic environmental gradient between the two knees of a wiggle does not necessarily associate with a decrease in the productivity of the species (Case et al., 2005). Hence, the effects of wiggles on species' range dynamics can be essentially different from those of gradients in productivity.

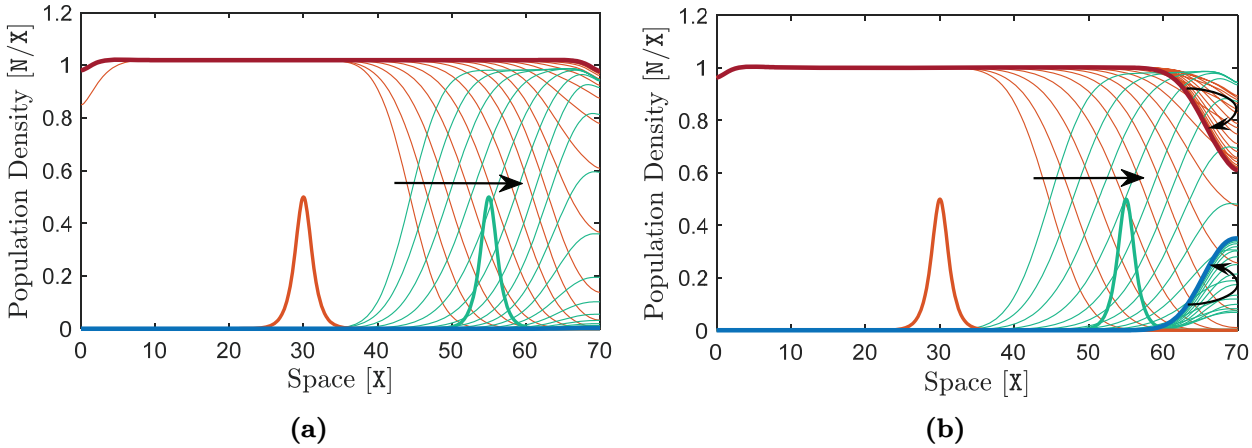

Figure 2: Competitive exclusion and marginal coexistence. Curves of population density of two competeing species are shown in each graph as their range evolves in time. Except for R_1 and R_2 which take different values in each graph, the rest of the model parameters for both species are the same and equal to the values given in Table 1. Arrows show the direction of evolution in time, after the region of sympathy is formed between the species and starts moving upward. The same description as given in Figure 1 holds for curve colors, and the highlighted curves in red and blue are the final curves obtained at the end of simulations. In (a) the downstream species is significantly stronger, with a maximum growth rate of $R_1 = 1.2\ \mathtt{T}^{-1}$ versus the growth rate $R_2 = 1\ \mathtt{T}^{-1}$ of the upstream species. Curves are shown at every 50 T for a simulation time horizon of $T = 1000\,\mathtt{T}$. The first species eventually excludes the second species from the habitat. In (b), the downstream species is still stronger, but less significantly than it is in (a), with $R_1 = 1.1\ \mathtt{T}^{-1}$ versus $R_2 = 1\ \mathtt{T}^{-1}$. Curves are shown at every 100 T for a simulation time horizon of $T = 5000\,\mathtt{T}$. The second species will be able to survive marginally at the vicinity of the habitat boundary. The curves of steady-state trait mean associated with each graph are shown in supplementary Figure S2.

To understand the range dynamics of two species as their competitively formed interface enters a wiggle, we first describe how gene flow affects range expansion of a solitary population in a linear environment. The population gradually expands its range as it becomes adapted to new environments under the force of natural selection. At the core of the population, the density of the population grows to the environment's maximum capacity and its trait mean converges to the environmental trait optimum. The population's density declines near the edge of its range, which creates an asymmetry in gene flow from the populous core of the population to its edge. Due to the presence of a gradient in trait optimum, the phenotypes that are pre-adapted at central regions of the range will be maladapted at peripheral regions. Therefore, the asymmetric gene flow decreases the mean fitness of the population at its range margins. As a result, population density decreases further near the range edge, which then results in a further increase in the asymmetry of gene flow. This positive feedback loop between population density and gene flow slows down the range expansion of the population.

It has been hypothesized that, when the environmental gradient is sufficiently steep, the asymmetric core-to-edge gene flow can eventually destabilize migration-selection balance and swamp local adaptation at range margins, thereby halting the species' range expansion (Haldane, 1956;

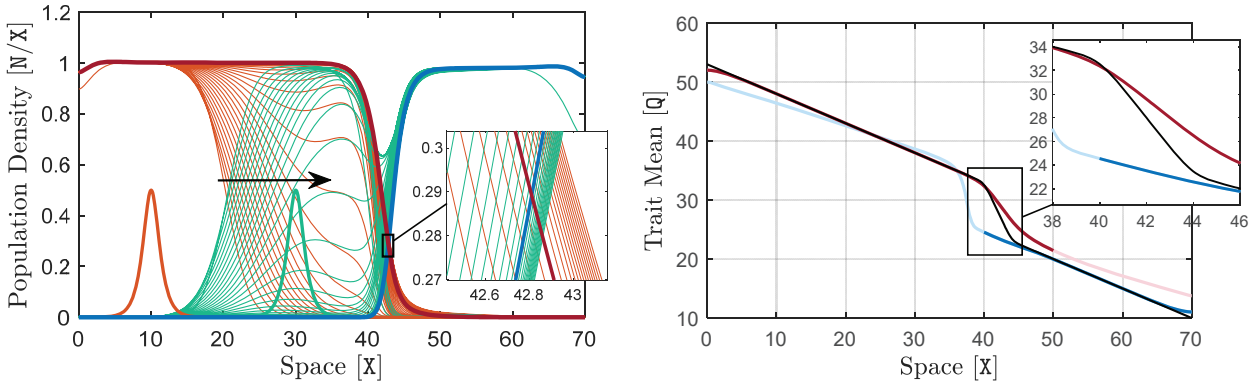

(a) **(b)**

Figure 3: Formation of stable range limits at an environmental wiggle. Here, $R_1 = 1.1\ \mathtt{T}^{-1}$, $R_2 = 1\ \mathtt{T}^{-1}$, and the rest of the parameters take their typical values given in Table 1. The simulation is performed for a time horizon of $T = 1000\ \mathtt{T}$ and curves of population density are shown in (a) at every 20 T. The same description as given in Figure 1 holds for the curve colors and the arrow. The highlighted curves in red and blue are associated with the time instance $t = 700\ \mathtt{T}$, when stable range limits are approximately formed at the environmental wiggle. The corresponding curves of trait mean at $t = 700\ \mathtt{T}$ are shown in (b). The black line in (b) shows the environmental trait optimum Q, whose slope switches sharply from $-0.5\ \mathtt{Q/X}$ to $-2.5\ \mathtt{Q/X}$ between the two knees of the wiggle located at $x = 40\ \mathtt{X}$ and $x = 44\ \mathtt{X}$, respectively. The curves of trait mean in (b) are made transparent over the regions where population densities are approximately zero.

Lenormand, 2002; Mayr, 1963). Under the assumption of constant trait variance, Kirkpatrick and Barton (1997) and Case and Taper (2000) have provided theoretical support for this hypothesis, particularly showing "range pinning" (stable localized range) in steep environmental gradients. However, letting the trait variance evolve jointly with the population density and trait mean, Shirani and Miller (2022) have shown that range pinning via genetic swamping is unlikely to occur in linear environments, no matter how steep their gradients are; see also (Barton, 2001). Gene flow along an environmental gradient inflates the trait variance; the steeper the gradient the higher the level of trait variation. Increased trait variation provides more "fuel" for natural selection to operate, which allows for local adaptation and range expansion even at exceedingly steep gradients. Yet, this does not imply population's survival at arbitrarily steep gradients. Natural selection imposes a phenotypic load on the mean growth rate of the population, which increases proportionally with the trait variance due to the term $-\frac{\mathrm{S}}{2}v$ in (7); note that we drop the enumeration index i when we only have one species in the habitat. If the gradient is too steep, the trait variance becomes too large and the population fails to survive under the excessive phenotypic load on its growth. Shirani and Miller (2022) find a maximum steepness of the gradient in trait optimum as $|\mathrm{d}_x\mathrm{Q}|_{\max} = \sqrt{(2\mathrm{R}^2/\mathrm{SD}) - \mathrm{U}/2\mathrm{D}}$, beyond which the population cannot survive in a linear environment (unless possibly marginally at the vicinity of the habitat boundary) and becomes extinct.

Based on the discussion above, we now note that wiggles with an exceedingly steep transition zone between their knees indeed appear as geographic barriers for species range expansion. For

the default parameter values given in Table 1, the maximum steepness $|\mathrm{d}_x \mathrm{Q}|_{\max}$ discussed above that still allows for survival will be equal to 3.16 Q/X. This means that, even in the absence of a competitor, a species will not be able to evolve to cross a wiggle in our simulations if the wiggle has a transition zone steeper than 3.16 Q/X. In our analysis below, we always consider shallower wiggles since geographic barriers are obvious causes of range limits and are not of particular research importance.

We now show that environmental wiggles can stabilize the range limits formed between two species, that are otherwise unstable in a completely linear environment. We simulate an environmental trait optimum that is linear everywhere with slope -0.5 Q/X except at a wiggle where its slope changes to -2.5 Q/X; see Figure 3b. We let the downstream species be stronger, with $\mathrm{R}_1 = 1.1\ \mathtt{T}^{-1}$ versus $\mathrm{R}_2 = 1\ \mathtt{T}^{-1}$. We initialize both species on the same side of the habitat, downstream to the wiggle, and let their range evolve for an evolutionary time horizon of $T = 1000$ T. The results are shown in Figure 3.

We first see in Figure 3a that the upstream species can expand its range indefinitely to the upstream habitat boundary. This particularly means that, despite the sharp transition in the steepness of the environmental gradient at the wiggle, the species is still able to adapt to and successfully cross the wiggle. At the wiggle, the range expansion of the species becomes significantly slower though, and the species fails to grow to its maximum capacity. These effects could be predicted based on the range dynamics of a solitary species that we described before. The very steep environmental gradient at the wiggle increases the maladpative effects of gene flow at the species' range margin and causes a strong phenotypic load that decreases the species' maximum density.

We further see in Figure 3a that the spatial distributions of the two species converge to an evolutionarily stable equilibrium. At this equilibrium, both species have a limited range and their range limit is established near the upstream knee of the wiggle. To understand the dynamics of this range limit formation, first note that a region of sympatry is initially created between the two species as they expand their range and meet each other. Since the downstream species is stronger, it pushes the interface between the two species toward the wiggle. When the species' interface enters the wiggle's transition zone, the substantially steeper environmental gradient of the wiggle intensifies the interactions between species' population density and gene flow. These interactions enhance the species' character displacement within the wiggle, sharpen the interface between the species, and slow down the advancement of the interface. The interface is eventually stabilized as an equilibrium near the upstream knee of the wiggle. The curves highlighted in red and blue in Figure 3a show the (approximate) population distribution of the spices at the equilibrium. Note that these curves are associated with the population distributions at $t = 700$ T and remain almost unchanged in the remaining 300 T of the simulation. The inset in Figure 3a helps better see the convergence of the range limits to an equilibrium.

The sharp change in steepness of the environmental gradient at the upstream knee of the wiggle is the key contributor to stabilization of the range limits. The steepness change at the downstream knee provides a further support for the stability of the limits. As the interface between the two

species approaches the upstream knee, the levels of asymmetric gene flow from central to peripheral populations of the two species change differently. The central population of the upstream species is pre-adapted to the outside environment adjacent to the upstream knee, which has a moderate slope. As a result, the peripheral population of this species suffers less of disruptive effects of gene flow as the interface approaches the upstream knee. By contrast, the central population of the downstream species is (partially) adapted to the steep gradient within the wiggle as well as the moderate gradient below the downstream knee. Therefore, the phenotypes that are brought by gene flow to a local peripheral population of the downstream species are significantly greater than the average local phenotype. As a result, the trait mean of the downstream species significantly deviates (upward) from the trait optimum near the upstream knee, causing a substantial fitness load on the peripheral population of this species. The curves of trait means in Figure 3b show the resulting difference between the (steady-state) local adaptation of the peripheral populations of the two species. Since competition between the two species takes place within their overlapping peripheral populations, the advantage that the downstream species gains from reduced maladpative effects of gene flow eventually compensates for its competition weakness. This balances the competition between the two species and stabilizes their range limits as an equilibrium near the upstream knee.

In principle, when the downstream species is competitively stronger, a single environmental knee such as the upstream knee in Figure 3—across which the slope of the environment changes from steep to moderate—is sufficient for stabilizing the range limits. This is provided the difference between the slopes is sufficiently large. To see this, we repeat the simulation associated with Figure 3 but with a wiggle with much wider transition zone (and hence not actually called a wiggle by our definition), so that the downstream knee has no contribution to stabilization of the limits. The downstream species can successfully adapt to the steep zone of the environment, but since its peripheral population still suffer more of the disruptive effects of asymmetric gene flow compared with the upstream species, it loses its competition advantage near the upstream knee. The resulting evolutionary stable range limits are shown in supplementary Figure S3. It should be noted though, that in nature, such a steep environmental gradient is unlikely to be successfully colonized by a species over such a wide geographic zone. Other factors, such as Allee effects, will likely contribute to prevent the advancement of the species over the steep gradient. The presence of a downstream knee in a wiggle, in short distance to the upstream knee, not only makes the wiggle more plausible to exist in nature, but also contributes to stabilization of the range limits. This is because the downstream species can grow to high density in the moderate gradient below the downstream knee. Since the wiggle is relatively short, the disruptive effects of asymmetric gene flow from the high-density core of this species still remains in effect in its peripheral population that is in competition with the other species near the upstream knee.

We conclude this section by a few remarks. In order for a wiggle to stabilize range limits, the difference between the steepness of the environmental gradient across the knees (particularly the upstream knee in the case where the downstream spices is stronger) must be sufficiently large. In addition, the maximum survival gradient $|\mathrm{d}_x\mathrm{Q}|_{\max} = \sqrt{(2\mathrm{R}^2/\mathrm{SD}) - \mathrm{U}/2\mathrm{D}}$ found by Shirani and Miller (2022) suggests that the range limits of slowly growing species under strong natural selection

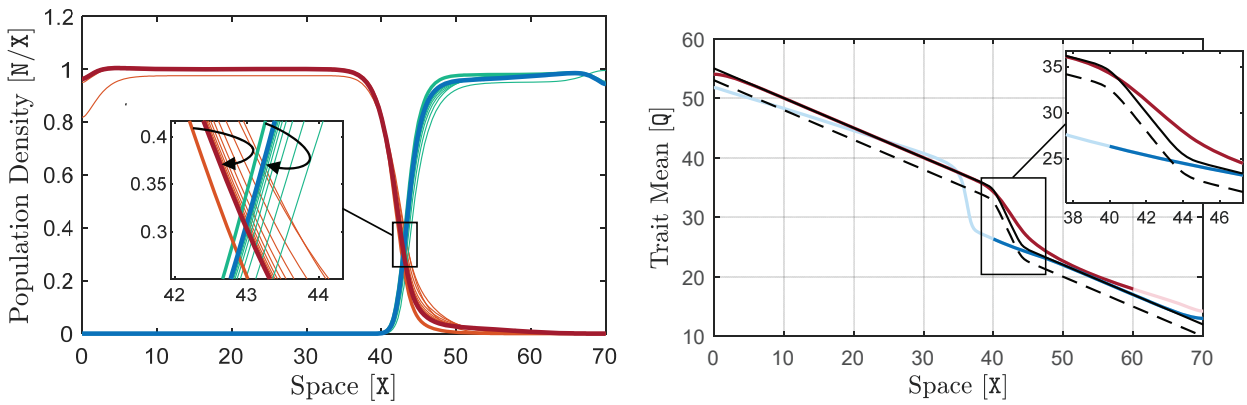

(a) **(b)**

Figure 4: Robustness of the stability of the range limits against moderate climatic perturbations. The simulation is performed using the same model parameters as in Figure 3. The highlighted curves obtained at $t = 700$ T in Figure 3 (when the stable range limits were formed) are used as the initial curves here. Starting from $t = 0$ T, the curve of trait optimum Q is gradually shifted up by a factor of 2 Q over a time course of 10 T and remains unchanged afterwards. The initial curve of Q is shown by the dashed black line in (b), and the completely shifted curve after $t = 10$ T is shown by the solid black line. The simulation is performed for a time horizon of $T = 200$ T. Curves of population density are shown at every 10 T in (a), and the final curves obtained at $t = 200$ T are highlighted. Correspondingly, the curves of trait mean obtained at $t = 200$ T are shown in (b). The same description as given in Figure 1 holds for the curve colors. We observe that the range limits remain stable under the climate-warming perturbation applied at the beginning of the simulation.

can be stabilized by wiggles with shallower transition zones. Our simulation results shown in Figure S4 also imply that, when competition between the species is more intensive (larger values of V_i), the range limits can be stabilized by a shallower wiggle. Finally, we note that the convergence of the species' range limits to a stable equilibrium at the wiggle, as in Figure 1a, is fairly independent of the initial arrangements of the populations. Figure S5 shows that the range limits can similarity be stabilized at a wiggle even if the two species are initialized at opposite sides of the wiggle.

Climate Change and Stability of the Range Limits

The stability of the range limits formed as a coevolutionary equilibrium at wiggles is robust against sufficiently small climatic perturbations. Here, we show the robustness against sustained climate-warming perturbations. The robustness against cooling perturbations can be shown similarly. We initialize our simulation with the two equilibrium populations of Figure 3 whose range limits have been stabilized at the wiggle. To simulate a climate-warming perturbation, we then gradually shift up the curve of trait optimum Q by a factor of 2 Q over a time course of 10 T, starting from the beginning of the simulation. When the course of climate warming is complete, we fix the curve of Q at its new profile until the end of the simulation. We allow the species to evolve for $T = 200$ T. The results are shown in Figure 4. At the beginning, both species suffer some population losses as they

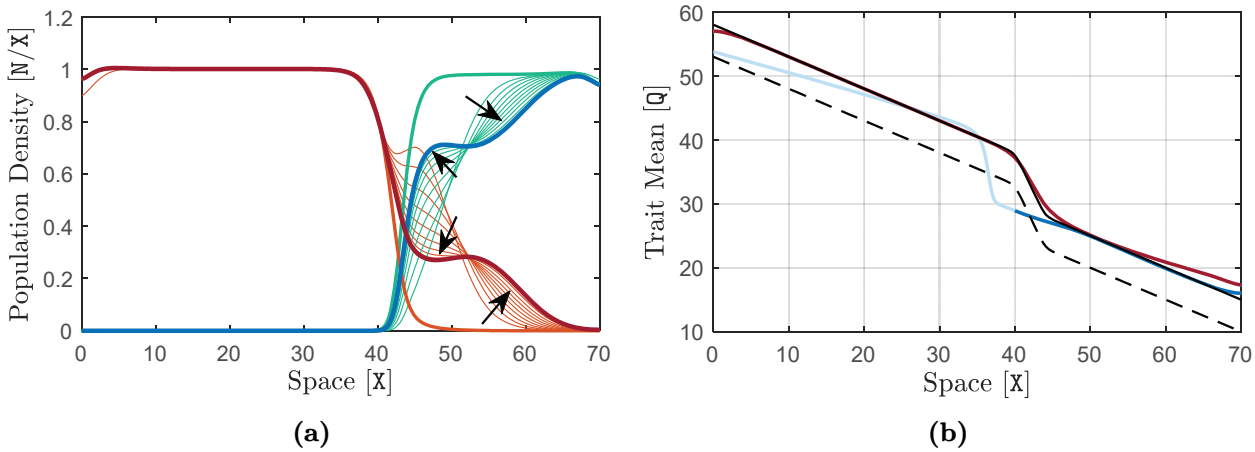

Figure 5: Destabilization of the range limits by strong climate warming when the downstream species is stronger. The same simulation as presented in Figure 4 is performed here, with the only difference being that the shift in the trait optimum takes a larger magnitude of 5 Q. The curves of population density are shown in (a) at every 20 T, up to the time $t = 200$ T. The final curves are highlighted in red and blue at $t = 200$ T, and their corresponding trait mean curves are shown in (b). The same description as given in Figure 4 holds for curve colors and the dashed curve. Arrows indicate the direction of evolution in time. Due to the larger magnitude of climate warming, the initially stable range limits are destabilized, which results in an upslope expansion in the stronger species' range. Further continuation of the simulation up to $T = 1000$ T is shown in supplementary Figure S6, which demonstrates the possibility of a limited existence of the weaker species at the vicinity of the wiggle.

fail to fully adapt to the changing environment. Since the peripheral population of the (stronger) downstream species initially has trait mean values greater than the environmental optimum within the wiggle (particularly near the upstream knee of the wiggle where the range limits get stabilized), this population suffers less from the incremental changes in the optimum phenotype. As a result, the range limits of the two species are slightly pushed upslope by this spices when climate warming is taking place. However, once the warming is complete and both species successfully adapt to the new environment, the range limits return to their initial equilibrium state. This confirms the robustness of the stability of the range limits against the climatic perturbation we simulated here.

Climate warming can destabilize the stable range limits of Figure 3 if it is sufficiently large in magnitude and occurs sufficiently fast. To see this, we repeat the same simulation as described above (Figure 4), but with a stronger climate-warming perturbation of magnitude 5 Q. The evolution of the species' range for 200 T is shown in Figure 5a. Here, the advantage that the peripheral population of the (stronger) downstream species has—due to its partial pre-adaptation to larger phenotype values within the wiggle—is significant enough to allow this species push the range limits entirely out of the wiggle, before the upstream spices finds a chance to sufficiently adapt to the warming climate. As a result, the range limits become destabilized and the downstream species succeeds in crossing the wiggle and expanding its range.

In general, there are several possibilities for the future range evolution of the species (with the

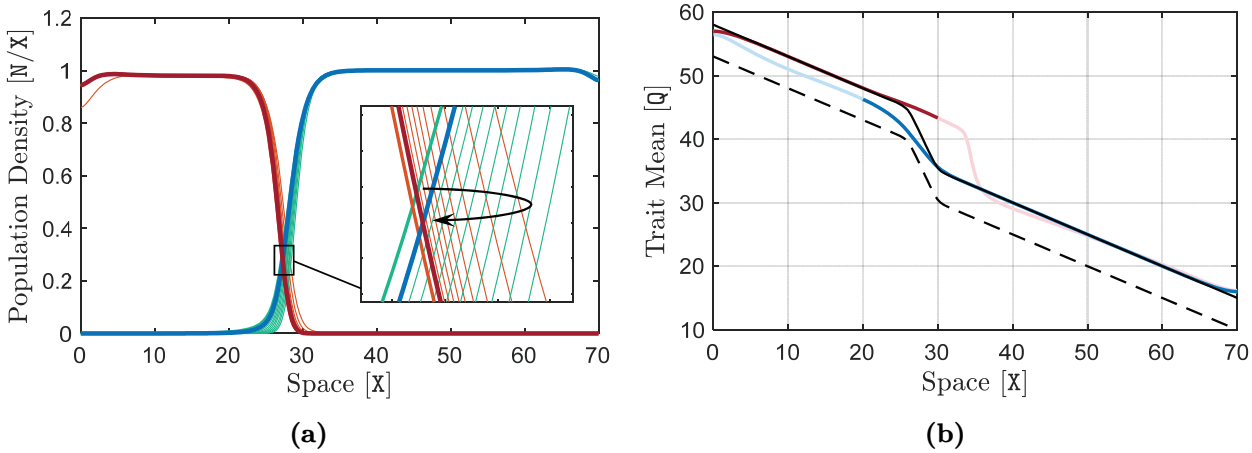

Figure 6: Robustness of the stability of the range limits against strong climate warming when the upstream species is stronger. Here, $R_1 = 1\ \mathtt{T}^{-1}$ and $R_2 = 1.1\ \mathtt{T}^{-1}$, that is, in contrast with the results shown in Figure 3, the upstream (green) species is made stronger here. The rest of the parameters take their typical values given in Table 1. The environmental wiggle occurs over the interval $[26\,\mathtt{X}, 30\,\mathtt{X}]$. The formation of the stable range limits at the wiggle is shown in the supplementary Figure S7. Similar to the results shown in Figure 5, the highlighted curves obtained at $t = 700\ \mathtt{T}$ in Figure S7 (when the stable limits are formed) are used as the initial curves here, and the curve of trait optimum Q is gradually shifted up by a factor of 5 Q over the time interval from 0 T to 10 T. The simulation is performed for a time horizon of $T = 200\ \mathtt{T}$ and curves of population density are shown in (a) at every 20 T. The final curves obtained at $t = 200\ \mathtt{T}$ are highlighted in red and blue, and their corresponding trait mean curves are shown in (b). The same description as given in Figure 5 holds for the curve colors, the dashed curve, and the arrow. We observe that, unlike the case where the downstream species was stronger (Figure 5), the range limits remain stable even though the climate-warming perturbation is fairly large in magnitude.

downstream species being stronger) when their range limits formed at a wiggle is destabilized by climate warming. If there is another wiggle upstream to the previous wiggle, then the species' range can possibly get limited and stabilized by the new wiggle. In this case, the strong climate-warming perturbation indeed causes an upslope shift in species' range limits from one wiggle to another wiggle. In the absence of another wiggle, the stronger species may eventually exclude the weaker one entirely from the habitat, or the spices' distribution may converge to an evolutionarily stable state of marginal coexistence at the vicinity of the habitat boundary; such as the state shown in Figure 2. Our further continuation of the simulation of Figure 5 up to $T = 1000\ \mathtt{T}$ revealed another, less intuitive, possibility. The results are shown in supplementary Figure S6. We see that the species' ranges converge to an evolutionarily stable equilibrium. At this equilibrium, the stronger species occupies the entire available habitat, and the weaker species survives at the vicinity of the wiggle with a low density and limited range.

Finally, we show that if the upstream species is stronger, then the stability of the range limits formed at a wiggle is robust even against strong climate warming perturbations. For this, we repeat the simulations of Figures 3 and 5, but this time with $R_2 = 1.1\ \mathtt{T}^{-1}$ versus $R_1 = 1\ \mathtt{T}^{-1}$. That is, we first initialize the two spices at one side of a wiggle and let their ranges be stabilized

at the wiggle. The results are shown in Figure S7. We then use the equilibrium populations of this simulation to initialize the second simulation, where we apply a strong climate warming perturbation of magnitude 5 Q, like what we did in Figure 5, and let the species' ranges evolve for $T = 200$ T. The results are shown in Figure 6. Similar to what we saw in Figure 5a, during climate warming the range limits are (slightly) pushed upslope by the downstream species whose peripheral population is partially pre-adapted to larger phenotypes. However, since this species is competitively weaker here, it cannot push the range limits outside the wiggle. Even if it can, possibly due to a stronger warming perturbation, the stronger upstream species will eventually push the limits back again to their original equilibrium in the wiggle (once the course of climate warming is complete and both species become adapted to the new climate).

Discussion

Models of Interspecific Competition and Range Limits

Previous theoretical studies have established that interspecific competition can limit species' ranges (Case and Taper, 2000; Case et al., 2005; Goldberg and Lande, 2007; Price and Kirkpatrick, 2009; Roughgarden, 1979; Shirani and Miller, 2022; Tilman, 1982). The models used in these studies may or may not incorporate adaptive evolution, movements across space, and environmental heterogeneity. The non-evolutionary models often include additional factors for setting range limits, such as anti-correlated spatial profiles for species' carrying capacity, or abrupt shifts in species' dominance based on their resource utilization dynamics. However, when two species are similar enough to undergo strong competition, then it is also expected that they have similar resource utilization dynamics and respond similarly to the abiotic environment (Case et al., 2005). Moreover, non-evolutionary models cannot address the possibility that a species may evolve to release itself from the constraining impacts of the other. Therefore, these models cannot verify whether or not the established range limits will be evolutionarily stable (Price and Kirkpatrick, 2009). Among the studies that consider adaptive evolution, the work of Price and Kirkpatrick (2009) particularly proposes that interspecific competition can set evolutionarily stable range limits even in the absence of disruptive effects of gene flow, and even in the case where species are competitively nonidentical. However, their analysis does not include species' movement. As a result, it overlooks the possibility that the established range limits might indeed move in space due to the difference between competition strengths of the species, leaving doubts on the stability of the range limits as they propose.

The model developed by Case and Taper (2000) still remains as one of the most comprehensive evolutionary models that demonstrates stable range limits set by the interactions between interspecific competition and gene flow. However, we argued that their analysis still suffers from two major limitations: an unrealistic assumption of constant trait variance, and a conclusion on the stability of the range limits that is valid only for the non-generic case of identical competitors. We used an extension of Case and Taper's model (developed by Shirani and Miller (2022)) that allows

for trait variance to evolve. We analyzed the formation and stability of the range limits for the more general cases of nonidentical species, and showed how environmental "wiggles" can robustly stabilize the range limits.

Implications for Range Limits and Their Stability

The results we obtained have implications for the ongoing debate in ecology about how and when interspecific competition limits species' ranges (Paquette and Hargreaves, 2021; Soberón, 2007). We showed that the interaction between interspecific competition and gene flow along an environmental gradient can still limit species' ranges even when their trait variance is free to evolve. When the environmental trait optimum varies linearly, the range limits are generically unstable though: the overlap between the species constantly moves towards the weaker species. This may eventually lead to complete exclusion of the weaker species, or to an evolutionarily stable state at which this species marginally coexists with the dominant species at the vicinity of the habitat boundary. If the environment has a sufficiently steep wiggle (step-like nonlinearity) ahead of the moving overlap, then the moving limits eventually get stabilized at the wiggle. The stability of the range limits is robust against sufficiently small changes in climate. Whether or not the limits are destabilized by stronger climate changes depends on the type of the change (warming or cooling) and the relative position of the species across the wiggle. In our conceptualization of elevation-dependent temperature gradient (cooler at higher elevations), sufficiently strong climate-warming perturbations destabilize the range limits when the downstream species is dominant, allowing this species to cross the wiggle and make an upslope expansion in its range. However, the stability of the range limits is robust even against strong climate-warming perturbations when the upstream species is dominant. Opposite effects hold for climate-cooling perturbations.

Environmental Nonlinearities and Range Limits in Nature

The importance of interspecific competition in limiting species' ranges in nature is ultimately an empirical question, but our theoretical results shed light on this question. In particular, we highlight the crucial role of steep changes or wiggles along environmental gradients in determining where interspecific competition can set stable range limits. Nonlinearities along environmental gradients, such as wiggles, would seem to be common in empirical systems. For example, ecotones between habitats are commonly observed. Some empirical observations also support an important role for step-like changes in environmental gradients to stabilizing species' range limits. For example, closely related species often share a common range border at ecotones (Bull, 1991; Terborgh, 1985) and other transitional locations along environmental gradients (Mauro et al., 2021); consistent with the predictions of our analysis.

Species' Response to Climate Change

Our results provide a perspective on how climate change will lead to changes in species' ranges (Pecl et al., 2017). Most species are currently shifting poleward and upslope toward cooler environments,

but many species have stable ranges or are even shifting towards warmer conditions (Lenoir and Svenning, 2015; Lenoir et al., 2020). One possible explanation for these divergent responses to climate change is that species' interactions shape their ranges along environmental gradients. For example, interspecific competition between closely related species of tropical birds is an important factor limiting their elevational ranges (Freeman et al., 2019, 2022; Jankowski et al., 2010). The simple expectation is that species' ranges will shift upslope as environments get warmer. However, our results suggest that this would hold only if the downstream (lower-elevation) species is the dominant competitor. Empirical evidence demonstrates this is not always (or even usually) the case (Freeman, 2020). Therefore, our results emphasize the importance of considering competitive dominance between species when predicting changes in range limits. When the environmental trait optimum varies almost linearly, a stronger competitor can expand its range regardless of whether it is located downstream to the other species (leading to an upslope shift in ranges) or is located upstream to it (leading to a downslope shift in ranges). If the range limits of the species are already stabilized at an environmental wiggle, then climate warming (if strong enough) can only result in an upslope shift in ranges, and that occurs only when the downstream species is dominant. These findings particularly support the importance of measuring competitive ability empirically (Alexander et al., 2015; Martin and Ghalambor, 2024; Sakarchi and Germain, 2023), as an important factor predicting species' responses to climate change.

References

J. M. Alexander, J. M. Diez, and J. M. Levine. Novel competitors shape species' responses to climate change. *Nature*, 525(7570):515–518, 2015. doi: 10.1038/nature14952.

N. Barton. Adaptation at the edge of a species range. In J. Silvertown and J. Antonovics, editors, *Integrating ecology and evolution in a spatial context*, chapter 17, page 365–392. Blackwell, Oxford, 2001.

N. H. Barton. Clines in polygenic traits. *Genetical Research*, 74(3):223–236, 1999. doi: 10.1017/S001667239900422X.

J. R. Bridle and T. H. Vines. Limits to evolution at range margins: when and why does adaptation fail? *Trends in Ecology & Evolution*, 22(3):140–147, 2007. doi: 10.1016/j.tree.2006.11.002.

C. M. Bull. Ecology of parapatric distributions. *Annual Review of Ecology, Evolution, and Systematics*, 22:19–36, 1991. doi: 10.1146/annurev.es.22.110191.000315.

T. J. Case and M. L. Taper. Interspecific competition, environmental gradients, gene flow, and the coevolution of species' borders. *The American Naturalist*, 155(5):583–605, 2000. doi: 10.1086/303351.

T. J. Case, R. D. Holt, M. A. McPeek, and T. H. Keitt. The community context of species' borders:

ecological and evolutionary perspectives. *Oikos*, 108(1):28–46, 2005. doi: 10.1111/j.0030-1299.2005.13148.x.

J. H. Connell. The influence of interspecific competition and other factors on the distribution of the barnacle chthamalus stellatus. *Ecology*, 42(4):710–723, 1961. doi: https://doi.org/10.2307/1933500.

J. H. Connell. On the prevalence and relative importance of interspecific competition: Evidence from field experiments. *The American Naturalist*, 122(5):661–696, 1983. doi: 10.1086/284165.

C. R. Darwin. *On the Origin of Species by Means of Natural Selection, or, the Preservation of Favoured Races in the Struggle for Life.* London: John Murray, 1859.

J. M. Diamond. Laboratory experiments, field experiments, and natural experiments. In J. M. Diamond and T. J. Case, editors, *Community Ecology*, pages 3–22. New York: Harper & Row, 1985.

P. W. Dillingham, J. E. Moore, D. Fletcher, E. Cortés, K. A. Curtis, K. C. James, and R. L. Lewison. Improved estimation of intrinsic growth rmax for long-lived species: integrating matrix models and allometry. *Ecological Applications*, 26(1):322–333, 2016. doi: 10.1890/14-1990.

B. G. Freeman. Lower elevation animal species do not tend to be better competitors than their higher elevation relatives. *Global Ecology and Biogeography*, 29(1):171–181, 2020. doi: doi.org/10.1111/geb.13014.

B. G. Freeman, J. A. Tobias, and D. Schluter. Behavior influences range limits and patterns of coexistence across an elevational gradient in tropical birds. *Ecography*, 42(11):1832–1840, 2019. doi: https://doi.org/10.1111/ecog.04606.

B. G. Freeman, M. Strimas-Mackey, and E. T. Miller. Interspecific competition limits bird species' ranges in tropical mountains. *Science*, 377(6604):416–420, 2022. doi: 10.1126/science.abl7242.

K. J. Gaston et al. *The structure and dynamics of geographic ranges.* Oxford University Press, Oxford, 2003.

E. Goldberg and R. Lande. Ecological and reproductive character displacement on an environmental gradient. *Evolution*, 60(7):1344–1357, 2006. doi: 10.1111/j.0014-3820.2006.tb01214.x.

E. Goldberg and R. Lande. Species' borders and dispersal barriers. *The American Naturalist*, 170 (2):297–304, 2007. doi: 10.1086/518946.

N. G. Hairston. The experimental test of an analysis of field distributions: Competition in terrestrial salamanders. *Ecology*, 61(4):817–826, 1980. doi: 10.2307/1936752.

J. B. S. Haldane. The relation between density regulation and natural selection. *Proceedings of the Royal Society of London. Series B - Biological Sciences*, 145(920):306–308, 1956. doi: 10.1098/rspb.1956.0039.

J. E. Jankowski, S. K. Robinson, and D. J. Levey. Squeezed at the top: Interspecific aggression may constrain elevational ranges in tropical birds. *Ecology*, 91(7):1877–1884, 2010. doi: https://doi.org/10.1890/09-2063.1.

M. Kirkpatrick and N. H. Barton. Evolution of a species' range. *The American Naturalist*, 150(1): 1–23, 1997. doi: 10.1086/286054.

J. Lenoir and J.-C. Svenning. Climate-related range shifts – a global multidimensional synthesis and new research directions. *Ecography*, 38(1):15–28, 2015. doi: doi.org/10.1111/ecog.00967.

J. Lenoir, R. Bertrand, L. Comte, L. Bourgeaud, T. Hattab, J. Murienne, and G. Grenouillet. Species better track climate warming in the oceans than on land. *Nature Ecology & Evolution*, 4(8):1044–1059, 2020. doi: doi.org/10.1038/s41559-020-1198-2.

T. Lenormand. Gene flow and the limits to natural selection. *Trends in Ecology & Evolution*, 17 (4):183–189, 2002. doi: https://doi.org/10.1016/S0169-5347(02)02497-7.

A. M. Louthan, D. F. Doak, and A. L. Angert. Where and when do species interactions set range limits? *Trends in Ecology & Evolution*, 30(12):780–792, 2015. doi: 10.1016/j.tree.2015.09.011.

R. Macarthur and R. Levins. The limiting similarity, convergence, and divergence of coexisting species. *The American Naturalist*, 101(921):377–385, 1967. doi: 10.1086/282505.

P. R. Martin and C. K. Ghalambor. Is competitive ability the key adaptation to benign environments? Revisiting experiments on closely related species of tidal plants. *Biology Letters*, 20(5): 20230509, 2024. doi: 10.1098/rsbl.2023.0509.

A. A. Mauro, J. Torres-Dowdall, C. A. Marshall, and C. K. Ghalambor. A genetically based ecological trade-off contributes to setting a geographic range limit. *Ecology Letters*, 24(12):2739–2749, 2021. doi: https://doi.org/10.1111/ele.13900.

E. Mayr. *Animal Species and Evolution.* Harvard University Press, Cambridge, MA, 1963.

T. E. X. Miller, A. L. Angert, C. D. Brown, J. A. Lee-Yaw, M. Lewis, F. Lutscher, N. G. Marculis, B. A. Melbourne, A. K. Shaw, M. Szűcs, O. Tabares, T. Usui, C. Weiss-Lehman, and J. L. Williams. Eco-evolutionary dynamics of range expansion. *Ecology*, 101(10):e03139, 2020. doi: 10.1002/ecy.3139.

C. Niel and J. Lebreton. Using demographic invariants to detect overharvested bird populations from incomplete data. *Conservation Biology*, 19(3):826–835, 2005. doi: 10.1111/j.1523-1739.2005.00310.x.

A. Paquette and A. L. Hargreaves. Biotic interactions are more often important at species' warm versus cool range edges. *Ecology Letters*, 24(11):2427–2438, 2021. doi: https://doi.org/10.1111/ele.13864.

G. T. Pecl, M. B. Araújo, J. D. Bell, J. Blanchard, T. C. Bonebrake, I.-C. Chen, T. D. Clark, R. K. Colwell, F. Danielsen, B. Evengård, L. Falconi, S. Ferrier, S. Frusher, R. A. Garcia, R. B. Griffis, A. J. Hobday, C. Janion-Scheepers, M. A. Jarzyna, S. Jennings, J. Lenoir, H. I. Linnetved, V. Y. Martin, P. C. McCormack, J. McDonald, N. J. Mitchell, T. Mustonen, J. M. Pandolfi, N. Pettorelli, E. Popova, S. A. Robinson, B. R. Scheffers, J. D. Shaw, C. J. B. Sorte, J. M. Strugnell, J. M. Sunday, M.-N. Tuanmu, A. Vergés, C. Villanueva, T. Wernberg, E. Wapstra, and S. E. Williams. Biodiversity redistribution under climate change: Impacts on ecosystems and human well-being. *Science*, 355(6332):eaai9214, 2017. doi: 10.1126/science.aai9214.

T. D. Price and M. Kirkpatrick. Evolutionarily stable range limits set by interspecific competition. *Proceedings of the Royal Society B: Biological Sciences*, 276(1661):1429–1434, 2009. doi: 10.1098/rspb.2008.1199.

J. Roughgarden. *Theory of Population Genetics and Evolutionary Ecology: An Introduction.* Macmillan, New York, 1979.

J. Sakarchi and R. M. Germain. The evolution of competitive ability. *The American Naturalist*, 201(1):1–15, 2023. doi: 10.1086/722234.

T. W. Schoener. Field experiments on interspecific competition. *The American Naturalist*, 122(2): 240–285, 1983. doi: 10.1086/284133.

J. P. Sexton, P. J. McIntyre, A. L. Angert, and K. J. Rice. Evolution and ecology of species range limits. *Annual Review of Ecology, Evolution, and Systematics*, 40(1):415–436, 2009. doi: 10.1146/annurev.ecolsys.110308.120317.

F. Shirani and J. R. Miller. Competition, trait variance dynamics, and the evolution of a species' range. *Bulletin of Mathematical Biology*, 84(3):37, 2022. doi: 10.1007/s11538-022-00990-z.

J. Soberón. Grinnellian and eltonian niches and geographic distributions of species. *Ecology Letters*, 10(12):1115–1123, 2007. doi: https://doi.org/10.1111/j.1461-0248.2007.01107.x.

J. Terborgh. The role of ecotones in the distribution of andean birds. *Ecology*, 66(4):1237–1246, 1985. doi: doi.org/10.2307/1939177.

D. Tilman. *Resource competition and community structure.* Princeton University Press, 1982.

A. R. Wallace. *The Geographical Distribution of Animals: With a Study of the Relations of Living and Extinct Faunas as Elucidating the Past Changes of the Earth's Surface.* New York: Harper & Brothers, 1876.

M. S. Wisz, J. Pottier, W. D. Kissling, L. Pellissier, J. Lenoir, C. F. Damgaard, C. F. Dormann, M. C. Forchhammer, J.-A. Grytnes, A. Guisan, R. K. Heikkinen, T. T. Høye, I. Kühn, M. Luoto, L. Maiorano, M.-C. Nilsson, S. Normand, E. Öckinger, N. M. Schmidt, M. Termansen, A. Timmermann, D. A. Wardle, P. Aastrup, and J.-C. Svenning. The role of biotic interactions in shaping

distributions and realised assemblages of species: implications for species distribution modelling. *Biological Reviews*, 88(1):15–30, 2013. doi: https://doi.org/10.1111/j.1469-185X.2012.00235.x.

Environmental "Wiggles" as Stabilizers of Species Range Limits Set by Interspecific Competition (Supplementary Figures)

Farshad Shirani* Benjamin G. Freeman†

*School of Mathematics, Georgia Institute of Technology, Atlanta, GA 30332, USA
†School of Biological Sciences, Georgia Institute of Technology, Atlanta, GA 30332, USA

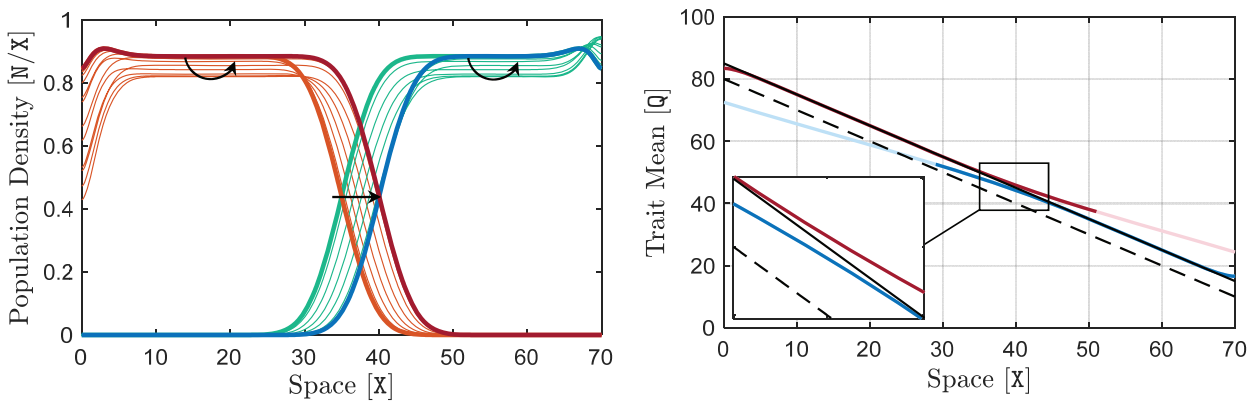

(a) **(b)**

Figure S1: Permanent shift in the equilibrium region of sympatry and range limits in response to a sustained climate-warming perturbation. The two species are competitively identical, with the same parameters as used in Figure 1 in the main text. The species are initialized at $t = 0$ T by the final solution curves (equilibrium state) obtained at the end of the simulation associated with the upper panel of Figure 1 (with $\nabla_x \mathrm{Q} = -1$ Q/X). Starting from $t = 0$ T, the curve of trait optimum Q is gradually shifted up by a factor of 5 Q over a time course of 10 T, and remains unchanged afterwards. The initial curve of Q is shown by the dashed black line in (b), and the completely shifted curve after $t = 10$ T is shown by the solid black line. The simulation is performed for a time horizon of $T = 200$ T. Curves of population density are shown at every 10 T in (a) and the final curves obtained at $t = 200$ T are highlighted. The curves of trait mean obtained, correspondingly, at $t = 200$ T are shown in (b). The same description as given in Figure 1 of the main text holds for the curve colors and arrows. We observe that the range limits converge to a new equilibrium state after the climate-warming perturbation takes place, resulting in an upslope shift in range limits and the region of sympatry.

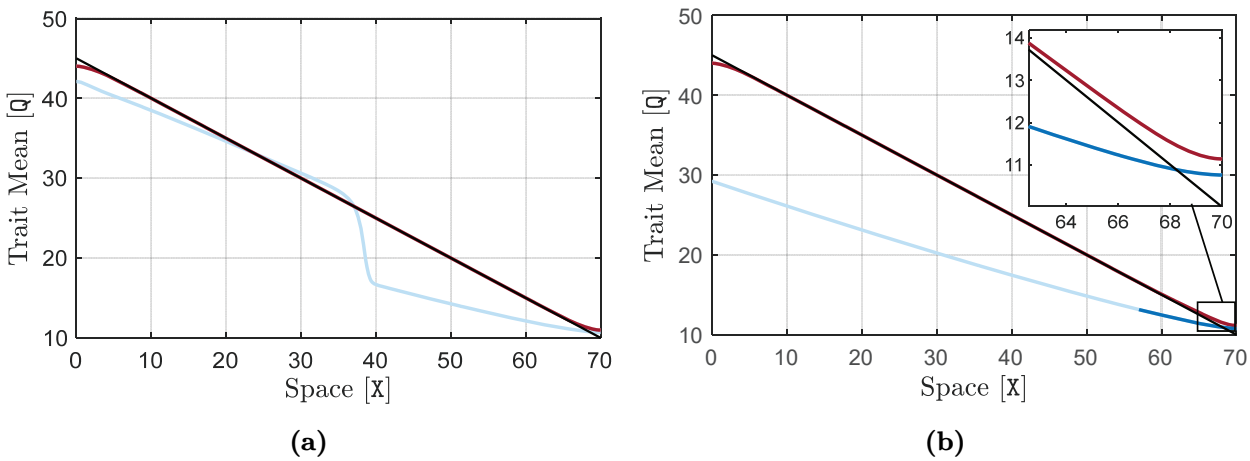

Figure S2: Steady-state trait mean of the populations associated with competitive exclusion and marginal coexistence regimes. The curves of steady-state trait means associated with the simulations shown in Figure 2 of the main text are shown here. Graph (a) shows the steady-state trait means for the competitive exclusion regime of Figure 2a, where $R_1 = 1.2\ \mathtt{T}^{-1}$ and $R_2 = 1\ \mathtt{T}^{-1}$. Graph (b) shows the steady-state trait means for the marginal coexistence regime of Figure 2b, where $R_1 = 1.1\ \mathtt{T}^{-1}$ and $R_2 = 1\ \mathtt{T}^{-1}$. For the upstream species in (b), which exists with a limited range, the trait mean curve is made transparent over the region where the population density is approximately zero.

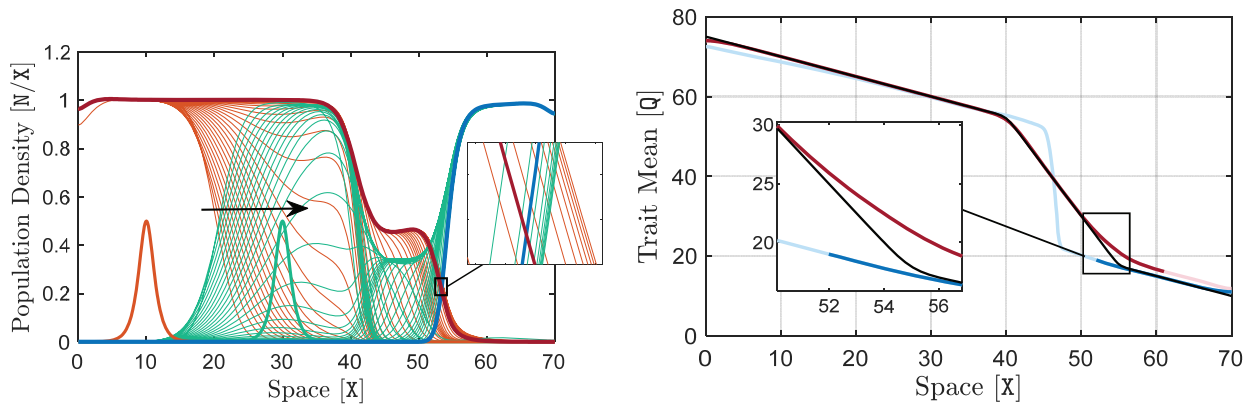

(a) **(b)**

Figure S3: Formation of stable range limits at an environmental knee. The same simulation as in Figure 3 of the main text is repeated here, but with a wiggle with much wider transition zone (and hence not actually called a wiggle based on our definition). Therefore, the downstream knee has no contribution to stabilization of the limits. Specifically, $R_1 = 1.1\ \mathtt{T}^{-1}$, $R_2 = 1\ \mathtt{T}^{-1}$, and the rest of the parameters take their typical values given in Table 1. The simulation is performed for a time horizon of $T = 1000\ \mathtt{T}$, and curves of population density are shown in (a) at every 20 T. The same description as given in Figure 1 of the main text holds for the curve colors and the arrow. The highlighted curves in red and blue are associated with the time instance $t = 850\ \mathtt{T}$, when stable range limits are approximately formed near the upstream knee. The corresponding curves of trait mean at $t = 850\ \mathtt{T}$ are shown in (b). The black line in (b) shows the environmental trait optimum Q, whose slope switches sharply from $-0.5\ \mathtt{Q}/\mathtt{X}$ to $-2.5\ \mathtt{Q}/\mathtt{X}$ between the two knees of the wiggle located at $x = 40\ \mathtt{X}$ and $x = 55\ \mathtt{X}$, respectively. The curves of trait mean in (b) are made transparent over the regions where population densities are approximately zero, as the values of trait mean over these regions are not biologically meaningful.

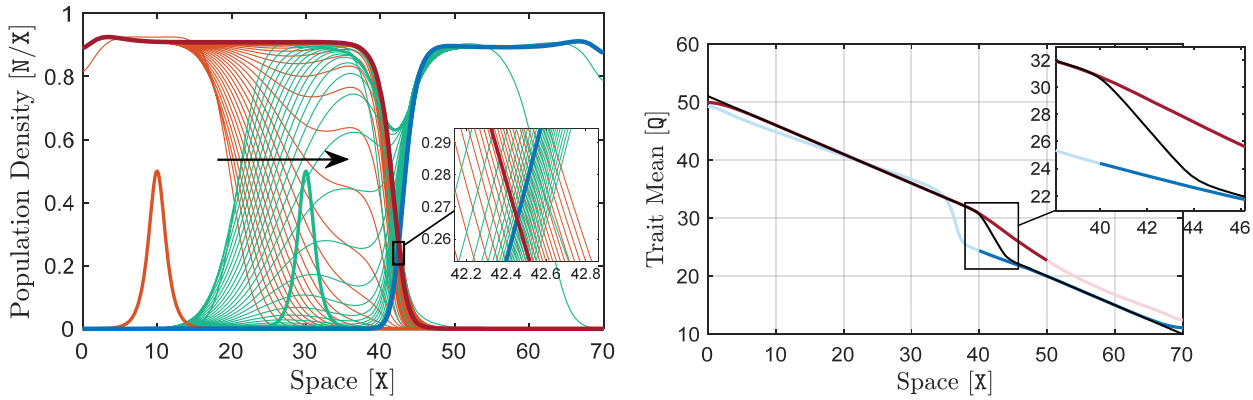

(a) **(b)**

Figure S4: Formation of stable range limits at an environmental wiggle when the wiggle's transition zone is less steep but interspecific competition is strong. The same simulation as in Figure 3 of the main text is repeated here, but for more generalist species with $V_1 = V_2 = 10$ $\mathtt{Q}^2$ (which implies stronger interspecific competition) and a less steep wiggle. The simulation is performed for a time horizon of $T = 1000$ $\mathtt{T}$ and curves of population density are shown in (a) at every 20 $\mathtt{T}$. The same description as given in Figure 1 of the main text holds for the curve colors and the arrow. The highlighted curves in red and blue are associated with the time instance $t = 700$ $\mathtt{T}$, when stable range limits are approximately formed at the environmental wiggle. The corresponding curves of trait mean at $t = 700$ $\mathtt{T}$ are shown in (b). The black line in (b) shows the environmental trait optimum Q, whose slope switches sharply from -0.5 $\mathtt{Q}/\mathtt{X}$ to -2 $\mathtt{Q}/\mathtt{X}$ between the two knees of the wiggle located at $x = 40$ $\mathtt{X}$ and $x = 44$ $\mathtt{X}$, respectively. The curves of trait mean in (b) are made transparent over the regions where population densities are approximately zero, as the values of trait mean over these regions are not biologically meaningful.

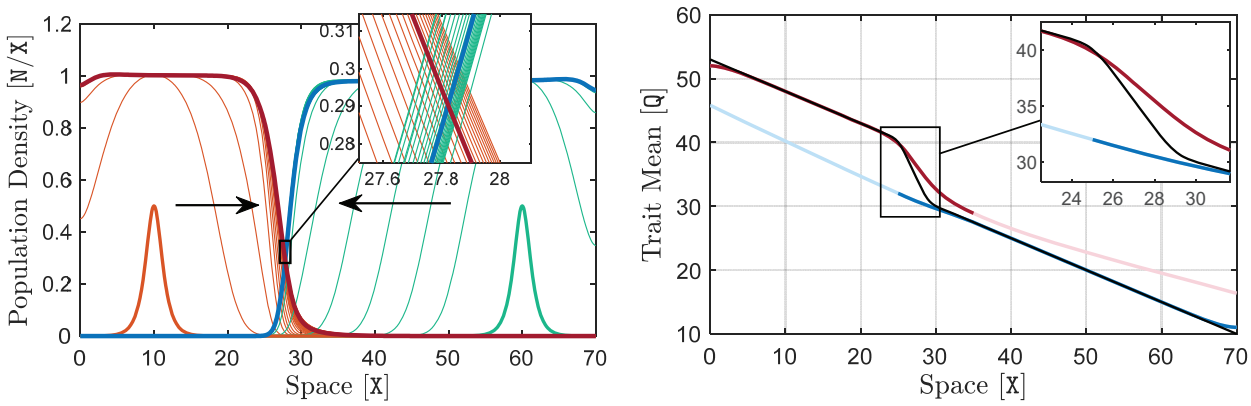

(a) **(b)**

Figure S5: Formation of stable range limits at an environmental wiggle when the two species are initialized at opposite sides of the wiggle. Here, $R_1 = 1.1\ \mathtt{T}^{-1}$, $R_2 = 1\ \mathtt{T}^{-1}$, and the rest of the parameters take their typical values given in Table 1. The simulation is performed for a time horizon of $T = 300\ \mathtt{T}$ and curves of population density are shown in (a) at every 10 T. The same description as given in Figure 1 of the main text holds for curve colors and arrows. The highlighted curves in red and blue are associated with the time instance $t = 200\ \mathtt{T}$, when stable range limits are approximately formed at the environmental wiggle. The corresponding curves of trait mean at $t = 200\ \mathtt{T}$ are shown in (b). The black line in (b) shows the environmental trait optimum Q, whose slope switching sharply from $-0.5\ \mathtt{Q/X}$ to $-2.5\ \mathtt{Q/X}$ between the two knees of the wiggle located at $x = 25\ \mathtt{X}$ and $x = 29\ \mathtt{X}$, respectively. The curves of trait mean in (b) are made transparent over the regions where population densities are approximately zero, as the values of trait mean over these regions are not biologically meaningful.

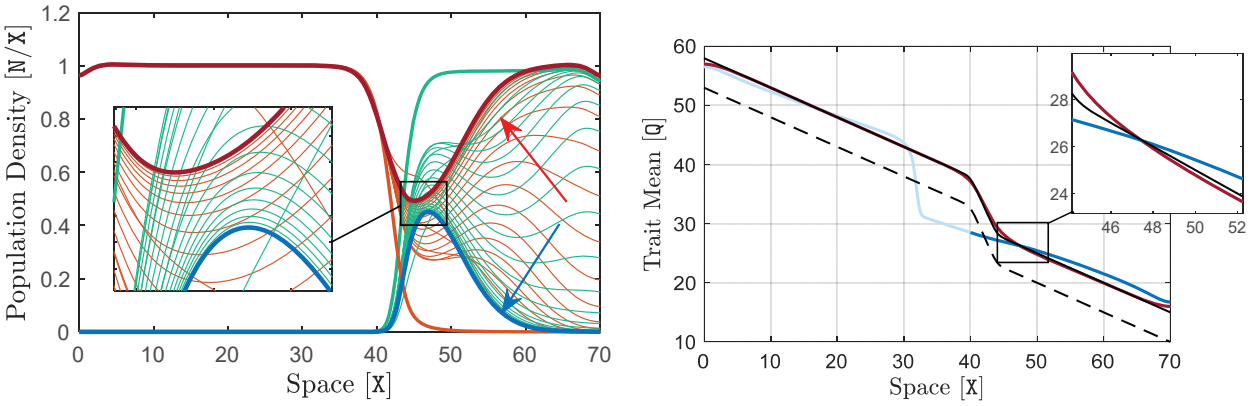

(a) **(b)**

Figure S6: Destabilization of the range limits by strong climate warming leading to an evolutionary stable limited sympatry. The same simulation as presented in Figure 5 of the main text is further continued here until a longer evolution time of $T = 1000$ T. Curves of population density are shown in (a) at every 50 T. The final curves are highlighted in red and blue at $t = 1000$ T and their corresponding trait mean curves are shown in (b). The same description as given in Figure 4 of the main text holds for curve colors and the dashed curve. The red arrow indicates the direction of evolution in time for the downstream (stronger) species, and the blue arrow indicates the direction of evolution for the upstream species. We see that the species' ranges converge to an evolutionarily stable equilibrium state, at which the weaker species survives over a limited region of sympatry with the stronger species at the vicinity of the wiggle. The mechanism of the formation of this equilibrium state can be explained as follows. The interspecific competition and the steep gradient of the wiggle jointly act to limit the range of the weaker species from the downstream (left) side. Due to the moderate slope of the environment outside the wiggle, the stronger species grows there to a high density. Hence, it competitively excludes the weaker species from the majority of the habit outside the wiggle. However, as the weaker species' range contracts against the wiggle, it suffers less of intraspecific competition and maladaptive core-to-edge gene flow. These advantages eventually balance the competition between the two species and an equilibrium state of limited sympatry is formed.

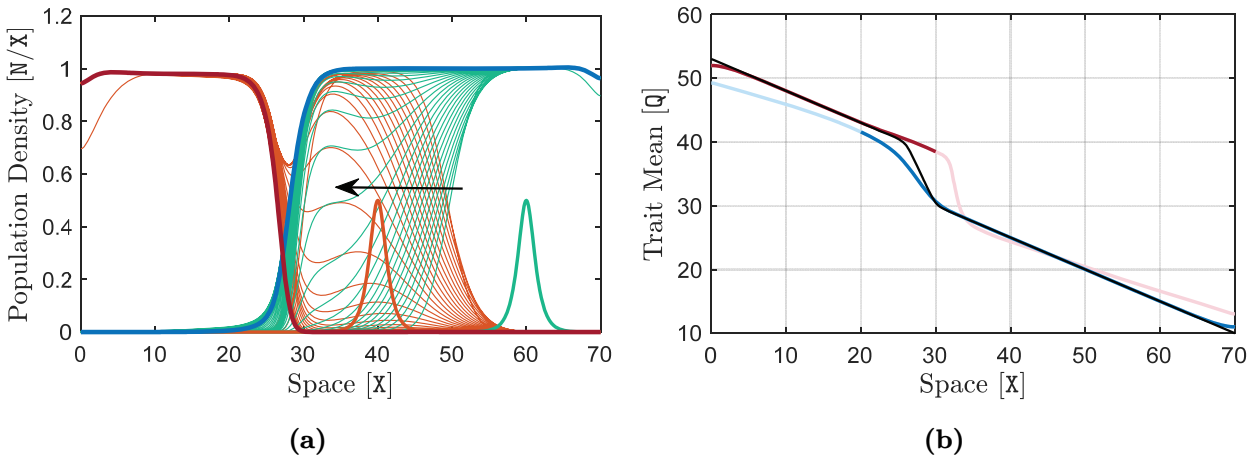

Figure S7: Formation of stable range limits at an environmental wiggle when the upstream species is stronger. A similar simulation to that presented in Figure 3 of the main text is performed here, with the main difference being that here the upstream species is made stronger. That is, we set $\mathrm{R}_1 = 1\ \mathtt{T}^{-1}$ and $\mathrm{R}_2 = 1.1\ \mathtt{T}^{-1}$. The rest of the parameters take their typical values given in Table 1. The simulation is performed for a time horizon of $T = 1000\ \mathtt{T}$ and curves of population density are shown in (a) at every 20 T. The same description as given in Figure 1 of the main text holds for the curve colors and the arrow. The highlighted curves in red and blue are associated with the time instance $t = 700\ \mathtt{T}$, when stable range limits are approximately formed at the environmental wiggle. The corresponding curves of trait mean at $t = 700\ \mathtt{T}$ are shown in (b). The black line in (b) shows the environmental trait optimum Q, whose slope switching sharply from $-0.5\ \mathtt{Q}/\mathtt{X}$ to $-2.5\ \mathtt{Q}/\mathtt{X}$ between the two knees of the wiggle located at $x = 26\ \mathtt{X}$ and $x = 30\ \mathtt{X}$, respectively. The curves of trait mean in (b) are made transparent over the regions where population densities are approximately zero, as the values of trait mean over these regions are not biologically meaningful.